Coadsorption of hydrogen and CO on Pt(335): Structure and vibrational Stark effect

Hong Wang and R. G. Tobin
Department of Physics and Astronomy and Center for Fundamental Materials Research, Michigan State University, East Lansing, Michigan 48824-1116

David K. Lambert
Physics Department, General Motors Research and Development Center, Warren, Michigan 48090-9055

(Received 6 April 1994; accepted 17 May 1994)

We have studied CO and H coadsorbed on the stepped Pt(335) surface in vacuum to learn about their interaction at steps and to compare with previous electrochemical studies. Both electroreflectance and conventional reflectance absorption vibrational spectra were obtained of atop bonded CO. Its stretch vibrational frequency ν, Stark tuning rate $(d\nu/dE)$, and integrated absorbance S were all studied as functions of CO and H coverage. With CO only on step edges, S for atop CO decreases to zero with increasing H coverage. The CO affected by H is in a mixed phase and is bridge bonded. Atop CO's $(d\nu/dE)$ decreases with increasing CO coverage but is unaffected by coadsorbed H. In the low CO coverage limit $(d\nu/dE)=88\pm9$ cm^{-1}/(V/Å), in agreement with theory and with previous measurement. The standard model of dipole–dipole screening is unable to explain the CO coverage dependence of both $(d\nu/dE)$ and S. The vibrational polarizability of CO increases with coverage. We also compare our results with spectroelectrochemical data from CO on Pt(335) in aqueous electrolyte. Our measured $(d\nu/dE)$ is too small to explain the variation of CO's ν with electrode potential ϕ in the electrochemical experiments if $(dE/d\phi)$ in the double-layer is taken from conventional models. The effect of coadsorbed H is also different; in vacuum H has no effect on CO's $(d\nu/dE)$ but in electrolyte, at low CO coverage, $(d\nu/d\phi)$ drops to zero at the potential where H adsorption begins.

I. INTRODUCTION

Important applications involve CO and H coadsorbed on Pt, both in a gas[1,2] and at the electrochemical double-layer. Our experiment studies CO and H coadsorbed on Pt(335) in vacuum with applied electric field. We use IR spectroscopy (electroreflectance and polarization modulation), temperature programmed desorption (TPD), and low energy electron diffraction (LEED). As shown in Fig. 1, Pt(335) consists of (111) terraces, four atoms wide, separated by monatomic (100) steps; Pt(S)[4(111)×(100)] in step-terrace notation. Adsorbed hydrogen dissociates on Pt surfaces.[3,4]

One motivation to study a highly stepped surface like Pt(335) is to understand the polycrystalline surfaces used in applications. Both CO and H preferentially bind at a step edge. At the low CO coverages discussed here, CO occupies only edge sites. We are also interested in how CO's response to electrostatic and IR fields is changed by coadsorbed H. Our data for CO and H on Pt(335) in vacuum are compared with spectroelectrochemical data obtained by Kim *et al.*[5,6] for CO and H on Pt(335) in aqueous electrolyte.

There have been previous studies of CO on Pt(335) in vacuum,[7–14] but not with coadsorbed H. However, CO has been coadsorbed with H on Pt(112) (Ref. 15) and Pt(997) (Ref. 16) in vacuum. Both surfaces are vicinal to (111) and differ from Pt(335) mainly in terrace width. In step terrace notation Pt(112) and Pt(997) are Pt(S)[3(111)×(100)] and Pt(S)[9(111)×(111)], respectively. Bridge CO coexists with atop CO on Pt(335) (Refs. 10–13) and on Pt(997) (Ref. 16) over a wide range of CO coverage, but bridge CO is found on Pt(112) only near saturation CO coverage.[17] In the present work we find another difference; on Pt(112), H causes low-coverage CO to phase separate into one-dimensional islands along the step edge, but on Pt(335) H and CO form a mixed phase along the step edge.

This paper is organized as follows. We first discuss the experiment and our results. Next, a structural model for CO and H on the step edge is proposed that explains our observations. This is followed by a discussion of how E-field and coadsorbates affect CO's vibrational spectrum. We consider both the vibrational Stark effect and chemical explanations. We also compare our observations with previous electrochemical data.

II. EXPERIMENT

Our experiments were carried out in an ultrahigh vacuum (UHV) chamber with a base pressure of 2×10^{-10} Torr. The sample was spot-welded to two Ta wires, which were also used for heating and cooling. The sample temperature T could be controlled between 100 and 1400 K. The sample was cleaned by cycles of Ar ion bombardment, reacting at 1000 K with 2×10^{-8} Torr O_2, and annealing at ~1300 K. The sample's cleanliness was checked by Auger spectroscopy before any IR spectra were taken. Also, to minimize the adsorption of residual hydrogen on the sample surface, both the cold trap at the bottom of the UHV system and the reservoir of the sample manipulator were filled with liquid N_2 before the sample was allowed to cool below 300 K. Cryopumping by the cold surfaces reduced the H_2 residual gas pressure by about a factor 3. During dosing and data taking, T was 103–108 K. The sample was dosed with CO or H_2 by simply leaking the gas into the chamber.

 0021-9606/94/101(5)/4277/11/$6.00

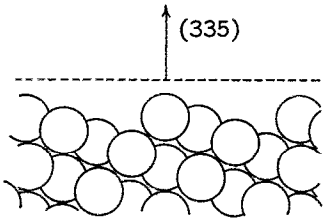

FIG. 1. Side view showing the atomic structure of the Pt(335) surface.

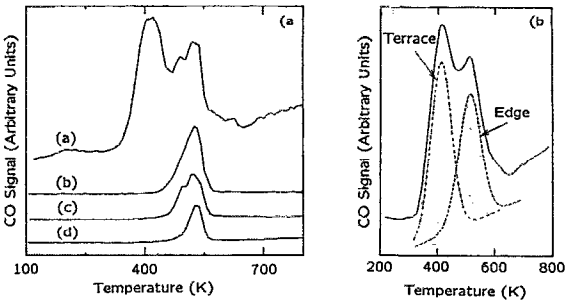

FIG. 2. (a) TPD spectra obtained by desorbing CO from the Pt(335) surface (without H). The CO dosages used to prepare (a)–(d) were 20, 1.5, 1.0, and 0.5 L, respectively. (b) Fit of two Gaussians (one from edge CO and the other from terrace CO) to the 20 L TPD spectrum.

Detailed descriptions of the spectroscopy techniques are given elsewhere.[18] A single lead–salt diode laser, with a spectral range of 1947–2022 cm^{-1}, was used as the IR source for both reflection–absorption IR spectroscopy (RAIRS) and electroreflectance vibrational spectroscopy (EVS). We used $^{13}C^{18}O$ for the experiment so the C═O stretch mode of atop CO could be seen with the laser; the frequencies characteristic of bridge-bonded CO were not accessible. The RAIR spectra were obtained using a photoelastic modulator to modulate the polarization of the light. The measured quantity in RAIRS is the fractional change $\Delta R/R$ in p-polarized reflectivity (actually the difference between p- and s-polarized reflectivity) induced by the adsorbate.

The EV spectra were taken by applying an oscillating (100 kHz) high voltage between the sample and a spherical counterelectrode, which created an oscillating electrostatic field normal to the surface. The measured quantity in EVS is S_E, the rms amplitude of the induced oscillation in reflectivity to p-polarized light, normalized by reflectivity. To interpret EV spectra quantitatively, the applied field must be known. The applied field depends on the applied potential and the sample-to-electrode distance. The sample-to-electrode distance was determined by measuring capacitance.[19]

The data discussed here were obtained on three different days, each with a fixed CO coverage. The angle of incidence of the light on the Pt(335) crystal was the same for both RAIRS and EVS on a given day. On the three days it was 86.4°, 86.4°, and 85.9°, and the rms static E-field at the surface was $\langle E\rangle=(3.1\pm0.2)$, (2.6 ± 0.2), and $(3.0\pm0.2)\times10^4$ V/cm, ordered by increasing CO coverage. These values of $\langle E\rangle$ are the average, weighted by the intensity of the focused IR beam, over the illuminated area of the sample.[19]

The CO overlayer was prepared by dosing the sample at 105 K, annealing at 420 K to remove H adsorbed from the background, and cooling back to 105 K; this removed more than 95% of the H but only ~8% of the CO. During H_2 dosing T was 103–108 K and it was kept in this range until the IR spectra with the highest H coverage had been taken. One EV and one RAIR spectrum were measured at each H coverage; each pair of spectra took ~90 min. After the IR spectra at the highest H_2 dosage were completed, a TPD up to 420 K was used to quantify and remove the H. As before, the CO remained. The sample was then cooled back to 103–108 K, RAIR and EV spectra were taken, and the final CO coverage was measured with TPD.

We also performed experiments in which the overlayer was annealed 10 min at 198 K after H_2 dosing. This did not change the CO's IR spectra. Consequently, at the coverages studied, both CO and H are sufficiently mobile at ~100 K to reach their equilibrium configuration, in agreement with Luo *et al.*[11]

The CO and H coverages were referenced to the coverages obtained by dosing to saturation with CO or H_2 alone at 103–108 K. The saturation coverage of CO on Pt(335) is 0.63 ML.[9] (Here 1 ML is the coverage with an adsorbate on each surface atom of Pt.) The saturation coverage of H on Pt(S)[9(111)×(111)] is 1.0 ML.[20] We assume that the saturation coverage of H on Pt(335) is also 1.0 ML. The CO coverages on the three days were 0.06, 0.12, and 0.16 ML.

The intermediate H coverages studied with IR were determined in separate experiments by repeating the CO and H_2 dosing sequences and performing TPD for each dosage. The background exposure to H_2 (approximately 0.1 L) that took place during a pair of IR spectra (one EVS and one RAIRS) was accounted for in replicating the coverages. The final coverages obtained by repeating the dosing schedule agreed with the post-IR coverages. For example, with 1.5 L CO, the post-IR TPD gave $\theta_{CO}=0.16$ and $\theta_H=0.30$ ML. After the repeated dosing schedule, TPD gave $\theta_{CO}=0.15$ and $\theta_H=0.29$ ML. Here θ_{CO} and θ_H are the coverages of CO and H, respectively.

We also used LEED to search for possible reconstruction of the Pt(335) surface or the formation of ordered overlayers that might be caused by H and CO adsorption. No change from the clean surface was detected in the LEED pattern. In contrast, Pt(100) (Ref. 21) and Pt(110) (Ref. 22) do reconstruct, and an ordered CO overlayer is seen on Pt(112).[23]

III. EXPERIMENTAL RESULTS

A. TPD

Examples of TPD spectra for only CO on Pt(335) are shown in Fig. 2(a). The initial CO coverages were saturation and the three θ_{CO} studied with IR. The TPD peak at highest T is from CO at step edges.[7] The low-T peak is from CO on the terrace. With saturation θ_{CO}, our TPD spectrum taken at 10 K/s has peaks at 416 and 518 K, in agreement with previous studies.[7,11] To resolve the TPD curve into an edge peak

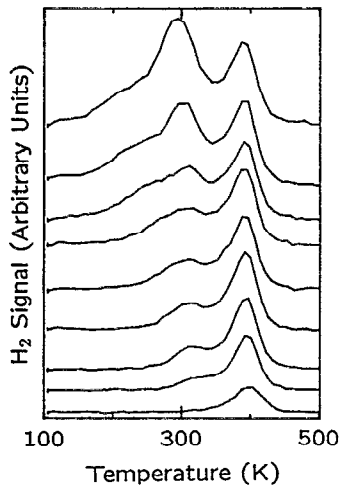

FIG. 3. TPD spectra obtained by desorbing H_2 from the Pt(335) surface (without CO). From top to bottom the dosages used to prepare the surface were 40, 20, 10, 3, 1.5, 0.8, 0.5, 0.3, and 0.1 L.

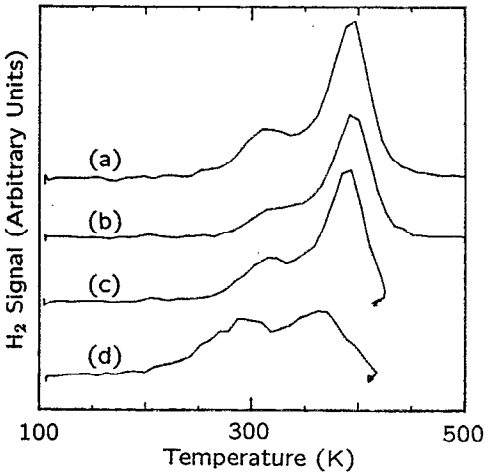

FIG. 4. TPD spectra obtained by desorbing H_2 from the Pt(335) surface (with and without CO). In (a) $\theta_{CO}=0$, $\theta_H=0.35$ ML; in (b) $\theta_{CO}=0$, $\theta_H=0.25$ ML; in (c) $\theta_{CO}=0.05$ ML, $\theta_H=0.31$ ML; and in (d) $\theta_{CO}=0.16$ ML, $\theta_H=0.30$ ML. The hydrogen doses were (a) 0.5 L; (b) 0.3 L; (c) 0.8 L; and (d) 4.5 L.

and a terrace peak they are modeled as Gaussians, as shown in Fig. 2(b). At saturation the edge peak is 40% of the total, in good agreement with Luo *et al.*[11] who found 43%. The TPD spectra in Fig. 2(a) show that at the CO coverages used for the IR spectra, without coadsorbed H, all of the CO was on the edge; none was on the terrace.

TPD spectra (10 K/s) for H alone on clean Pt(335) are shown in Fig. 3. At the lowest coverage there is one peak at 395 K. As θ_H increases, this peak stays fixed and a new peak appears at ~315 K. The new peak shifts to lower T with increasing θ_H. At high θ_H (0.8–1.0 ML) a third peak appears as a shoulder at ~250 K. At saturation θ_H, the fraction of the total area under the low, intermediate, and high-T peaks is 0.35, 0.39, and 0.26, respectively. With stepped Pt, the H_2 TPD peak at highest T is from chemisorbed H at edge sites.[24] Our data suggest that at saturation, 1/4 of the H is at edge sites, consistent with $\theta_H=1.0$ ML.

There have been previous TPD studies of H on stepped single-crystal Pt surfaces; Pt(S)[3(111)×(100)],[15,25] Pt(S)[6(111)×(100)],[26] Pt(S)[6(111)×(111)],[26] and Pt(S)[9(111)×(111)].[20] Surfaces with (100) oriented steps give H_2 TPD spectra with a high-T peak that dominates at low θ_H and a lower T peak with a shoulder that increases in area with increasing θ_H. Surfaces with (111) oriented steps give H_2 TPD spectra that are more difficult to separate into a "step" and "terrace" contribution if the surface is well annealed. For example, the β_2 peak and β_1 shoulder seen for high-θ_H desorption from Pt(S)[9(111)×(111)] (Ref. 20) are very similar to the β_2 peak and β_1 shoulder seen for high-θ_H desorption from Pt(111).[3] For Pt(111) Christmann *et al.*[3] have argued that the peak and shoulder both come from the same state—the peak is distorted because the binding energy of H varies with θ_H.

It is interesting to compare the H_2 TPD spectra of Pt(S)[n(111)×(100)] surfaces among Refs. 15, 20, 25, 26, and our experiments. The values of T at which desorption peaks occur in Refs. 20, 24, 25, and our experiments are generally consistent; in Ref. 15 the peaks are at lower T. In Refs. 20, 25, and 26 the TPD peak of H_2 from Pt(111) stays at ~330 K even though the heating rate ranged from 10 to 82 K/s. With low θ_H on Pt(S)[n(111)×(100)], our experiments and those in Refs. 20, 25, and 26 consistently find a peak at 400–430 K. As θ_H is increased, and H begins to occupy (111) terrace sites, a second peak appears at ~300 K. In contrast, Ref. 15 finds that for low θ_H on Pt(S)[3(111)×(100)], the peak is at 309 K, even lower than for H on Pt(111) in Refs. 20, 25, and 26. H on Pt(S)[3(111)×(100)] was also studied with TPD in Ref. 25; with low θ_H the peak was at 120 K higher than in Ref. 15. Only a small part of this discrepancy is due to heating rate (3.9 K/s in Ref. 15 and 67 K/s in Ref. 25); the faster heating rate is expected[27] to increase T at a first order peak ~35 K.

As shown in Fig. 4, predosed CO affects the TPD curves of H on Pt(335). As initial θ_{CO} increases, less θ_H results from a given H_2 dosage. Figure 5, which shows edge site occupancy by H vs H_2 dosage for three values of θ_{CO}, further illustrates this point. The interaction between coadsorbed H and CO is repulsive since increasing θ_{CO} monotonically reduces the T at which the H_2 TPD peak occurs.

The data in Fig. 4 show that at constant θ_H, an increase in predosed CO transfers H from edge to terrace sites (compare curves a and d). The TPD data taken in conjunction with IR spectroscopy were also analyzed to determine the occupancy of edge sites by CO and H. For all three CO coverages studied, after saturation with H, the total occupancy of CO and H at edge sites was 1.1±0.1. Each CO at an edge site blocks one site for H at the edge.

B. IR spectra

One set of EV and RAIR spectra ($\theta_{CO}=0.16$ ML) is shown in Fig. 6. The spectra taken at the other two θ_{CO} are similar. The resonant C–O stretch vibrational frequency vs

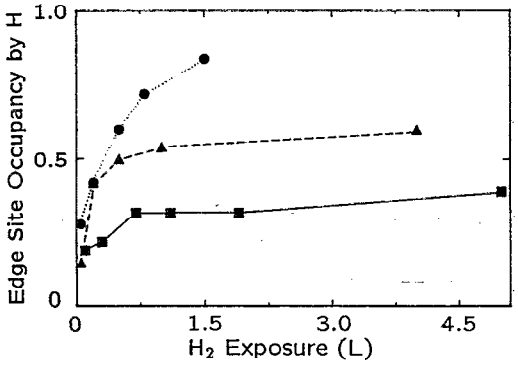

FIG. 5. Measured H occupancy of edge sites vs H_2 dosage with various precoverages of CO. The data with ●, ▲, and ■ were obtained by predosing with 0.5, 1.0, and 1.5 L of CO, respectively. The CO coverages were estimated from TPD to be 0.05, 0.10, and 0.16 ML, with CO occupying 0.18, 0.38, and 0.57 of the edge sites, respectively.

total θ_H is shown in Fig. 7, and the integrated RAIR intensity S is shown in Fig. 8. Both the EV and RAIR spectra were used to determine the resonant frequency. Smooth cubic splines were first interpolated through the data. Since the EV spectra are proportional to $d(\Delta R/R)/d\nu$, where $(\Delta R/R)$ is the RAIR signal and ν is optical frequency, the EV spectra were next integrated. The plotted peak frequency is the average from the RAIR and the integrated EV spectra.

The Stark tuning rate $(d\nu/dE)$ was determined by comparing the RAIR spectra with the integrated EV spectra. Two methods were used, comparison of peak heights and comparison of peak areas. The measured Stark tuning rate $(d\nu/dE)$ vs θ_H is plotted in Fig. 9 for each θ_{CO}. The data show that $(d\nu/dE)$ is independent of θ_H, but decreases with increasing θ_{CO}. The scatter in Figs. 7–9 comes largely from the ~2 cm^{-1} wide gaps that occur as the diode laser is tuned. When the spectrum has important structure in a gap—a peak

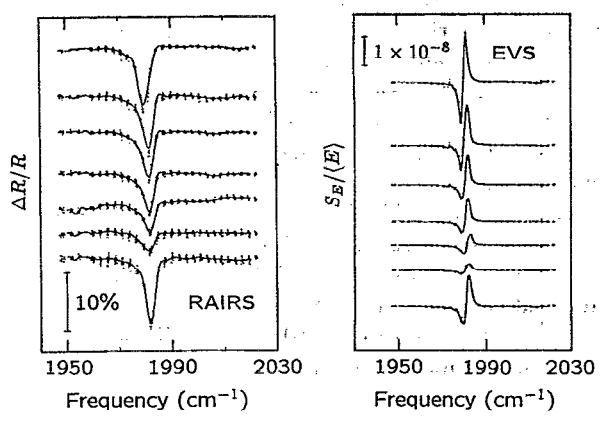

FIG. 6. RAIR and EV spectra of CO coadsorbed with H on Pt(335). The CO coverage was 0.16 ML for all of the spectra. From top to bottom the spectra are for θ_H=0.06, 0.10, 0.16, 0.18, 0.21, 0.29, and 0.06 ML. The lowermost spectrum was obtained after the sample had been heated to 420 K to desorb the H but leave the CO in place.

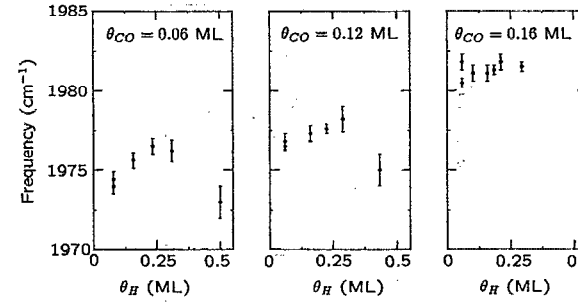

FIG. 7. Data showing the effect of coadsorbed H on the resonant frequency of the C–O stretch vibration at atop sites, for CO and H coadsorbed on Pt(335).

for example—information is lost. This is especially serious for EVS.

IV. STRUCTURAL MODEL OF THE CO+H OVERLAYER

Let us first recall what is known about CO adsorption on clean Pt(335). As CO's coverage builds up it occupies sites on the step edge first. Edge CO has a thermal desorption peak near 520 K (at 10 K/s) and an atop ν (for $^{12}C^{16}O$) between 2065 and 2080 cm^{-1}. As θ_{CO} continues to increase, terrace CO appears near 0.20 ML. Terrace CO has a thermal desorption peak near 420 K (at 10 K/s) and an atop ν between 2085 and 2100 cm^{-1}. At saturation (0.63 ML) all of the edge sites are occupied by atop CO, but on the terrace bridge and atop-bonded CO coexist.[5,6,10–13] Bridge CO at the edge is also present in an intermediate coverage range. A comprehensive model of CO buildup on Pt(335) was proposed by Luo *et al.*[11]

The experimental evidence from previous studies of CO and H coadsorption on Pt surfaces in vacuum[15,16,28–39] points convincingly toward a strongly repulsive CO–H interaction despite early claims[28,30,31] to the contrary. On Pt(111), even though the CO–CO interaction is repulsive, CO is pushed into islands of high density pure CO as θ_H increases.[36–38] On Pt(112), Henderson and Yates observed similar behavior.[15] They used electron-stimulated desorption ion angular distribution (ESDIAD) to monitor edge CO. The same sequence of structures was observed as θ_H was increased at fixed θ_{CO} as when θ_{CO} was increased at θ_H=0. This shows that H and

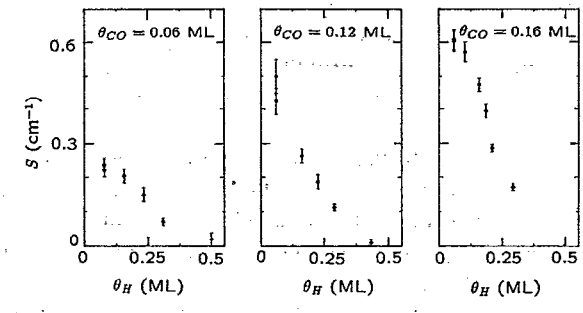

FIG. 8. Data showing the effect of coadsorbed H on integrated intensity S of the C–O stretch vibration at atop sites, for CO and H coadsorbed on Pt(335).

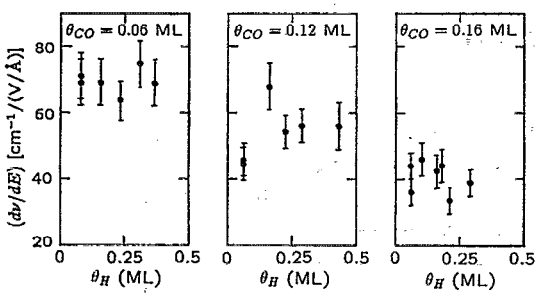

FIG. 9. Data showing the effect of coadsorbed H on the Stark tuning rate (dv/dE) of the C–O stretch vibration at atop sites, for CO and H coadsorbed on Pt(335).

CO form segregated one-dimensional islands along the step edge. As θ_H increases the CO is compressed.

Suppose that coadsorbed H and CO on Pt(335) also formed separate islands. An increase in θ_H should have the same effect on CO's IR spectrum as an increase in θ_{CO} at θ_H=0. As θ_H increases we would expect to observe (1) an increase in CO's resonant vibrational frequency ν; (2) little or no change in S; and (3) a reduction in $(d\nu/dE)$. Instead we see (Figs. 7–9) almost no change in ν, a strong reduction in S, ultimately to zero, and little or no change in $(d\nu/dE)$. Clearly, something different occurs on Pt(335), despite the strong structural similarity to Pt(112).

Our results are consistent with the following model: (1) Each CO blocks one H adsorption site; (2) H adsorbed at the edge forms compact one-dimensional islands of *mixed* H and CO, while within the H/CO islands, atop CO shifts to an adjacent edge bridge site; (3) Atop CO outside the H/CO islands is unaffected by θ_H.

On polycrystalline Pt there is previous evidence that *both* a mixed phase and islands occur.[34] The coadsorption of H and CO on single-crystal surfaces has been reviewed by White[32] and again by White and Akhter.[40] A mixed phase of H and CO has previously been observed on relatively open surfaces like Ni(100),[41,42] Ni(110),[43,44] Fe(100),[45] and Rh(100) (Ref. 46) near saturation coverage, but not on close-packed surfaces or at low coverage on any single-crystal surfaces. Our observation of a mixed phase for CO and H coadsorbed at a step edge, while unexpected, is generally consistent with previous experience. Sites at the edge are in an open environment. Also, even though the total coverage is below saturation the local coverage at the edge is still high; even at our lowest coverage, CO occupies 18% of the edge sites.

Assumption (1) follows from our TPD measurements (Sec. III A) which show that at saturation θ_H there is one adsorbate (H or CO) per edge atom for all three θ_{CO}.

Assumptions (2) and (3) explain the IR spectra. Figure 8 shows that increasing θ_H strongly reduces the IR intensity of atop CO. Our model explains this: the CO is being shifted to bridge sites, where its vibrational frequency lies outside the tuning range of our laser. A subsequent electron energy loss spectroscopy (EELS) experiment[47] has confirmed that the bridge CO coverage does increase with θ_H. The same effect has been observed in electrochemical experiments with coadsorbed CO and H on Pt(335),[5,6] and in vacuum experiments on Rh(100) (Ref. 46) and Ni(110).[43] Conversion of atop CO on the edge to bridge CO on the edge is also plausible on energetic grounds; with low θ_{CO} on Pt(111), atop CO is only 0.45 kcal/mol more strongly bound than bridge CO.[20]

Other explanations that we have considered for the disappearance of CO from the IR spectrum as H is coadsorbed on Pt(335) are less plausible. The CO does not move to atop sites on the terrace. Our IR spectra show that the terrace atop θ_{CO}<0.008 ML in the range of total θ_{CO} and θ_H discussed here. The inability of H to displace CO from edge to terrace sites is consistent with the known binding energies of CO and H at the two sites; edge CO is 5–8 kcal/mol more strongly bound than terrace CO (Refs. 14,15) but edge H is only 3 kcal/mol more strongly bound than terrace H.[24]

It is conceivable, but unlikely, that H causes a nearby CO to tilt nearly parallel to the surface (at least 77° from the surface normal to account for the observed loss of intensity). Tilted CO is commonly observed on stepped surfaces.[15,48–50] However, an explicit search[8] for tilted CO on Pt(335) found it to be vertical to within 10°. Even for CO on Pt(112), where CO does tilt,[15] the maximum tilt angle is only 20°.

Strong screening of the field at CO adsorption sites within islands is also unlikely. Generally, H adsorbs inside the image plane on metal surfaces.[51] On Pt(111) an explicit calculation shows that H is adsorbed at threefold hollow sites 0.95 Å above the topmost Pt layer.[52] For CO on Pt(111) the distance from the topmost Pt layer to the center of the CO molecule is 2.43 Å from LEED.[53] There are several ways to estimate where the image plane is on the Pt(111) surface.[54] They all suggest that the center of the CO bond is outside the image plane. We believe that edge atop CO on Pt(335) is a comparable distance from the topmost Pt atoms. Thus the center of the CO bond is at least 1 Å above the H layer. Both experiment and theory suggest that coadsorbed H does not significantly screen the local E-field at the CO adsorption site.

Reduction of CO's vibrational polarizability α_v by nearby H is ruled out. A reduction of α_v by at least a factor 20 would be required. However, the measured $(d\nu/dE)$ is expected to be proportional to $\sqrt{\alpha_v}$, so $(d\nu/dE)$ should drop by a factor 4.5 with increasing θ_H. Instead, Fig. 9 shows that $(d\nu/dE)$ does not change by more than ~20%.

Figures 7 and 9, which show the resonant frequency and $(d\nu/dE)$ of the atop CO that remains IR-active, demonstrate that this CO is unaffected by coadsorbed H, except at the very highest θ_H. In Sec. V B we estimate the θ_H-induced change in the local density of IR-active atop CO to be at most 0.02 ML. Since the total θ_{CO} on the edge remains constant with increasing θ_H, the average CO–CO distance in the mixed phase is about the same as in the pure phase—the mixed H/CO islands are *compact*. A uniform or random distribution of H atoms would lead to a *gradual* decrease of the frequency and a gradual increase in $(d\nu/dE)$ as the average distance between IR-active COs increased. Even though CO and H compete for sites, and the pairwise interactions are repulsive, the equilibrium state on the step edge has two

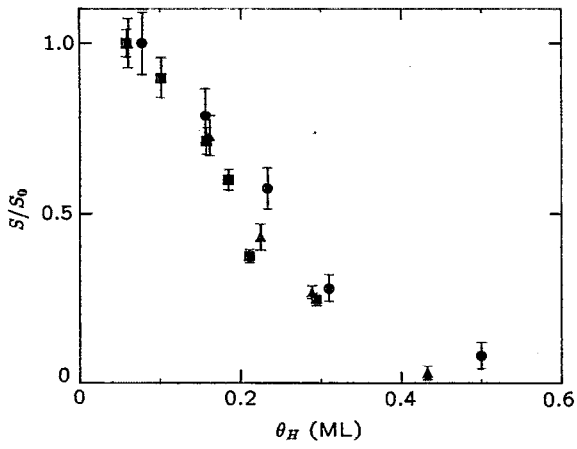

FIG. 10. Data showing the effect of coadsorbed H on the integrated intensity S for atop CO on Pt(335). With each CO coverage, the data have been normalized by S_0, the value of S at the lowest H coverage. The data with 0.06, 0.12, and 0.16 ML of CO are represented by ●, ▲, and ■, respectively.

phases—compact mixed islands and unaffected pure CO regions—with the same CO density in both.

Figure 10 provides further evidence that the local CO density is not affected by H. It shows S as a function of θ_H, *normalized to S at the lowest* θ_H. For all three θ_{CO}, a given θ_H eliminates the same *fraction* of the initial intensity, regardless of the initial θ_{CO}. If CO were expelled from growing H islands, more complicated behavior would be expected; one slope at low θ_H as the pure CO phase is compressed and a different, θ_{CO}-dependent slope at high θ_H as CO is incorporated into the growing H islands.

It is surprising that a mixed CO/H phase occurs on Pt(S)[4(111)×(100)] but that an island phase occurs on Pt(S)[3(111)×(100)] and on Pt(111). As discussed by White and Akhter,[40] in a situation with only pair interactions, a mixed phase between species A and B is energetically favored over an island phase if

$$\epsilon_{AB} < \tfrac{1}{2}(\epsilon_{AA} + \epsilon_{BB}). \tag{1}$$

Here ϵ_{AB} is the interaction energy between A and B, and similarly for ϵ_{AA} and ϵ_{BB}. Since H is inside the image plane, we do not expect its electrostatic interactions to be important. Generally, the strongest interaction between H and a coadsorbate on a metal is mediated by the metal's conduction electrons.

One explanation for the difference between the surfaces with three-atom and four-atom wide terraces is that molecules on adjacent terraces interact significantly, and this interaction changes the inequality in Eq. (1). In an extended Hückel calculation for CO and H on Rh(111), Ruckenstein and Halachev[55] showed that the through-metal interaction has a different dependence on separation for the CO–CO, H–H, and CO–H interactions. The length scale associated with the difference is a few lattice spacings. Although the computed energy difference is small, it could cause the observed change in going from three to four lattice spacings between edges.

Another explanation is that the local electronic structure near the edge is different on the two surfaces (without adsorbates), and this alters the interactions between adsorbates along an individual edge. A jellium calculation[56] shows that a single step has an associated dipole. The E-field from a line dipole decays as $1/d^2$, where d is the distance from the line. The induced surface charge at the nearest step consequently decreases by about a factor of 2 on going from Pt(112) to Pt(335). It is plausible that the extra charge could affect the CO–CO, H–H, and CO–H interactions differently, and this could change the equilibrium structure from a segregated phase to a mixed phase.

V. VIBRATIONAL STARK EFFECT AND COADSORBATES

A. Background

Our experiments directly measure the vibrational Stark effect; the effect of a static E-field on a molecule's vibrational spectrum. The Stark effect with externally applied E-field has also been studied theoretically. Quantum mechanics has been used to express $(d\nu/dE)$ for a molecule on a surface in terms of the molecule's dipole moment and potential energy functions.[19,57] (Here E is the *externally applied* electrostatic field.) The molecular properties needed for the calculation are measurable. There have also been *ab initio* calculations of $(d\nu/dE)$ for a single molecule on a surface[58–61] or in spatially uniform E-field.[62–68] In the limit of *low* adsorbate coverage the measurement-based and *ab initio* calculations of $(d\nu/dE)$ agree, and both have successfully predicted the directly measured $(d\nu/dE)$.[10,54] With *saturation* CO coverage on Ni(100) good agreement was also found.[19] With *high* coverage CO on Pt(111) and Pt(335), however, our previous experiments have found discrepancies between theoretical prediction and experiment.[9,10,54]

There are diverse experiments in which a change in static E-field affects ν. Examples include the "chemical" shift $\Delta\nu_{chem}$ vs adsorbate coverage for a homogeneous layer, $\Delta\nu$ induced by a coadsorbate, and $\Delta\nu$ induced by varying the substrate electrode's potential in an electrochemical cell. One of our motivations is to examine how well the vibrational Stark effect explains such data.

Many experiments[19] have found that $\Delta\nu$ is proportional to the change in local static field E_{loc},

$$\Delta\nu = \left(\frac{d\nu}{dE_{loc}}\right)\Delta E_{loc}. \tag{2}$$

For Eq. (2) to be useful, however, $(d\nu/dE_{loc})$ must be relatively insensitive to the environment, or at least the changes must be theoretically understood. For a single CO molecule on a metal surface, for example, theory predicts that $(d\nu/dE)$ is approximately proportional to the dipole moment derivative e^* so some account must be taken of the molecular environment.[69] Since e^* can be estimated from EELS or IR intensities, it is relatively straightforward to take its variation into consideration. If other molecular properties of CO var-

ied strongly with environment they would be more difficult to account for. There is evidence from an EELS experiment[14] that the important molecular properties of CO at edge and terrace sites on Pt(335) are similar, lending support to the usefulness of Eq. (2).

In a coadsorption experiment on a metal surface it is possible to monitor both ν and the work function Φ. For CO on Pt(111) both the chemical shift[70] $\Delta\nu_{\text{chem}}$ and the CO induced[71–73] $\Delta\Phi$ have been measured vs θ_{CO}. (Experimentally $\Delta\nu_{\text{chem}}$ is determined by varying the isotopic composition of the overlayer at constant total θ_{CO}.) At $T=125$ K, the measured $\Delta\nu_{\text{chem}}$ decreased from 0 at $\theta_{\text{CO}}=0$ to -10 cm^{-1} at $\theta_{\text{CO}}=0.33$ ML and then increased back to 0 at $\theta=0.5$ ML. Similarly, at 130 K the measured $\Delta\Phi$ decreased from 0 at $\theta_{\text{CO}}=0$ to -0.295 ± 0.038 eV at $\theta_{\text{CO}}\simeq0.33$ ML and then increased back to 0 at $\theta_{\text{CO}}\simeq0.5$ ML. (The θ_{CO} at which $\Delta\Phi$ returned to zero was 0.50 ML in Ref. 72 but 0.40 ML in Ref. 73.) Both $\Delta\nu_{\text{chem}}$ and $\Delta\Phi$ have the same functional form vs θ_{CO}. The proportionality constant between them is $(d\nu/d\Phi)=34\pm4$ cm^{-1}/eV.

Studies of CO on other metals have also suggested that $\Delta\nu\propto\Delta\Phi$. For CO on Ag, Yamamoto and Nanba[74] found that all the data of $\Delta\nu$ vs $\Delta\Phi$ with coadsorbed Xe, Kr, O, and Cl were described by a single linear correlation; $(d\nu/d\Phi)\sim45$ cm^{-1}/eV. For CO on Ni(111), Xu *et al.*[75] found that the data with coadsorbed O, CO, and Xe were described by $(d\nu/d\Phi)=35$ cm^{-1}/eV.

Electrochemical experiments with CO on Pt(111) have observed a similar effect.[76–86] Here, the potential ϕ of the Pt electrode relative to a reference electrode has been controlled directly while ν was measured with IR spectroscopy. Again, the data showed $\Delta\nu\propto\Delta\phi$. The measured $(d\nu/d\phi)$ depended on the solvent and solute of the electrolyte and on θ_{CO}. In aqueous 0.1 M $HClO_4$, with $\theta_{\text{CO}}=0.1$ and 0.65 ML, $(d\nu/d\phi)=45$ and 30 cm^{-1}/V, respectively, for the spectral line of atop CO. The close quantitative agreement between $(d\nu/d\Phi)$ for the chemical shift of CO on Pt(111) in vacuum and $(d\nu/d\phi)$ for CO at a Pt(111) electrode in an aqueous electrolyte suggests that they have a common origin.

Electrochemical experiments have tried to distinguish between $\Delta\phi$ and local E-field as the controlling variable for $\Delta\nu$ by varying either the solvent[84,85,87–92] or the solute[77,93–96] in the electrolyte. The observations are best explained if the controlling variable is the potential drop across the CO molecule—the local E-field—not just ϕ of the electrode.

However, other data suggest that $(d\nu/dE_{\text{loc}})$ varies significantly with local environment, and that Eq. (2), which focuses on E_{loc}, is less predictive than explicitly considering the chemical change of the molecule. In a study of CO on Rh(111) coadsorbed with Na, benzene, fluorobenzene, and ethylidyne, for example, Mate *et al.*[97] found that with equal concentrations of CO and the coadsorbate, $\Delta\nu$ was proportional to the coadsorbate's dipole moment. They also tried to estimate E_{loc} at the CO adsorption site. The correlation between $\Delta\nu$ and ΔE_{loc} was much worse than the correlation between $\Delta\nu$ and the coadsorbate's dipole moment.

A previous comparison[54] of the effect of θ_{CO} on S and $(d\nu/dE)$, for CO on Pt(111), also called into question the assumptions involved in using E_{loc} for predictive purposes. As we discuss in Sec. V B, $S\propto\theta_{\text{CO}}(\gamma_{\text{IR}}e^*)^2$, where γ_{IR} is an effective screening factor, and $(d\nu/dE)\propto\gamma_{\text{dc}}$, where γ_{dc} is the screening factor for the dc field. Within dipole coupling theory we expect $\gamma_{\text{dc}}\sim\gamma_{\text{IR}}$, so $(S/\theta_{\text{CO}})^{1/2}$ and $(d\nu/dE)$ should have the same dependence on θ_{CO} *even if* e^* *varies with coverage*. Experimentally[54] this is *untrue* for CO on Pt(111). A similar comparison for CO on Pt(335) is discussed in Sec. V B.

Comparison between the Stark effect measured in vacuum and electrochemical data also raises doubts about the transferability of $(d\nu/dE_{\text{loc}})$ in Eq. (2) from one situation to another. The vacuum experiments directly measure $(d\nu/dE)$. At low θ_{CO} in vacuum, screening (by both the adsorbates and the metal's conduction electrons) is expected to be negligible so $(d\nu/dE)$ should approach $(d\nu/dE_{\text{loc}})$. For CO on Pt(111) in the limit of low θ_{CO} in vacuum,[54] $(d\nu/dE)=75\pm9$ cm^{-1}/(V/Å).

In an electrochemical experiment the CO molecule is in the compact double-layer, and a model of the double-layer is required to relate ΔE_{loc} to change in electrode potential ϕ. There are many models of the double-layer. For an aqueous double-layer in the limit of low θ_{CO}, the model of Bockris *et al.*[98] implies that $(dE_{\text{loc}}/d\phi)=0.29$ (V/Å)/V. An alternative model—a CO monolayer—implies[19] that $(dE_{\text{loc}}/d\phi)=0.27$ (V/Å)/V. If we assume that the applied E-field is unscreened ($\gamma_{\text{dc}}=1$ or $E=E_{\text{loc}}$) at the CO molecule in the vacuum experiment then the Bockris model and the CO monolayer model imply that $(d\nu/d\phi)=22$ and 20 cm^{-1}/V, respectively, while the measured value at low CO coverage is 45 cm^{-1}/V. To use these models to explain the $(d\nu/d\phi)$ observed in the electrochemical experiments we would have to assume that $\gamma_{\text{dc}}\sim0.5$ at the CO adsorption site on Pt(111) in vacuum. This is too small to be explained by presently accepted theory.[54] (Early analyses[19,69] that obtained better agreement for electrochemical experiments with CO at Pt extrapolated from vacuum measurements with CO on Ni.[19,99])

These conflicting results lead us to consider theories that focus on chemical interaction, rather than E_{loc}. (These alternatives are not mutually exclusive. In some situations they are linked by the Hellmann–Feynman theorem.[100]) One chemical theory for the effect of coadsorbates on ν has been proposed by Ueba.[101] (Similar theories[102–104] had been proposed earlier.) Ueba starts with a Hamiltonian that includes the possibility of charge transfer between CO molecules, and between a CO molecule and the metal. Let $\Delta\nu$ be the difference between the observed ν at θ_{CO} and the singleton frequency. It consists of two parts, $\Delta\nu=\Delta\nu_{\text{dip}}+\Delta\nu_{\text{chem}}$, where $\Delta\nu_{\text{dip}}$ is from dipole–dipole coupling and $\Delta\nu_{\text{chem}}$ is from other effects. One prediction is that $\Delta\nu_{\text{chem}}\propto\Delta\Phi$, the change in Φ caused by adsorbing CO on the clean surface, consistent with the experimental results surveyed above. Another prediction is that CO's vibrational polarizability α_v increases with increasing θ_{CO}.

In the following sections we analyze our data for CO+H on Pt(335) to see whether it is best described by the vibrational Stark effect and E_{loc} or by chemical interactions. We find that the Stark effect theory accurately predicts $(d\nu/dE)$ at low coverage. However, the effect of coadsorbates is not readily explained by variations in E_{loc}. We also find qualita-

TABLE I. Summary of the IR spectra with only CO on Pt(335). Here θ_{CO} is the CO coverage, ν is the frequency of the peak in the IR spectrum, $(\Delta R)/R$ is the maximum CO-induced reflectivity change in the RAIR spectrum, $S=\int(\Delta R)/R\,d\nu$, and $(d\nu/dE)$ is the Stark tuning rate in terms of the externally applied E-field.

θ_{CO} (ML)	ν (cm^{-1})	$(\Delta R)/R$ (10^{-2})	S (cm^{-1})	$(d\nu/dE)$ [cm^{-1}/(V/Å)]
0.060±0.002	1974.4±0.5	4.8±0.3	0.24±0.02	88±9
0.120±0.004	1976.8±0.5	7.8±0.2	0.50±0.05	69±7
0.160±0.005	1981.8±0.5	13.8±0.3	0.61±0.03	52±5

tive support for Ueba's prediction of a coverage-dependent α_v.

B. Our experiment

The Stark tuning rate $(d\nu/dE)$ that we measured is given in Table I. Here E is the externally applied field. With only CO on clean Pt(335), our data generally agree with previous UHV studies.[7–13] In particular, we find that $(d\nu/dE)=88\pm9$ cm^{-1}/(V/Å) at low coverage (0.06 ML). In an earlier measurement at the same coverage in Ref. 9, $(d\nu/dE)=60\pm8$ cm^{-1}/(V/Å). There is also a theoretical relationship between $(d\nu/dE)$ and the measured IR cross section.[69] At this θ_{CO}, theory predicts[9] $(d\nu/dE)=70\pm11$ cm^{-1}/(V/Å). Theory and experiment are consistent at low CO coverage.

Dipole–dipole coupling is expected to affect the peak frequency ν, integrated intensity S, and Stark tuning rate $(d\nu/dE)$. Our data are shown in Table I. The variation of ν with θ_{CO} is largely explained by dipole–dipole coupling. We find that ν increases with θ_{CO} at 70 ± 5 cm^{-1}/ML. For comparison, Hayden *et al.*[7] found a slope of 52 cm^{-1}/ML for atop $^{12}C^{16}O$, corresponding to 48 cm^{-1}/ML for $^{13}C^{18}O$, significantly smaller than we observe. Both in our experiment and in Ref. 7, S increased nearly linearly with total θ_{CO} in this coverage range.

A linear increase of S with θ_{CO} at low θ_{CO} would ordinarily be expected. However, in the present experiment *not* all the CO is atop CO—a θ_{CO}-dependent fraction of it is bridge-bonded—so the linear relation between S and θ_{CO} is really a *nonlinear* dependence of S on the CO population being observed. Evidence that the bridge-bonded fraction of θ_{CO} increases with θ_{CO} comes both from EELS (Ref. 11) and IR (Refs. 12,13) experiments. The fraction of CO at atop sites is 1.0, 0.81, and 0.77 at $\theta_{CO}=0.06$, 0.12, and 0.16 ML, respectively. (These estimates come from Ref. 11, modified by recent evidence[47] that atop and bridge CO on the step edge have the same EELS intensity.) Since $S\propto\alpha_v$, one explanation for the data is that α_v *increases* with θ_{CO}. As total θ_{CO} increases from 0.06 to 0.16 ML, α_v would have to increase by >20% to keep S/θ_{CO} constant.

Other explanations that we have considered for the apparent increase in α_v with θ_{CO} are less plausible. The inclusion of dipole screening does cause a nonlinear dependence of S on θ_{CO}, but it has the wrong sign and only increases the need for α_v to increase with θ_{CO}. It would be possible to reconcile the data with a constant α_v if the ratio of bridge-to-atop CO was irreproducible: then all the CO could have been atop bonded in the present experiment and in Ref. 7, and only in Refs. 10–14 was part of it bridge bonded. Bridge-bonded CO was looked for and not seen with IR in Ref. 7. However, data from the EELS experiments is all consistent and the same crystal was used in the present experiment and in Refs. 9–14. An increase in α_v with θ_{CO} is the most likely explanation.

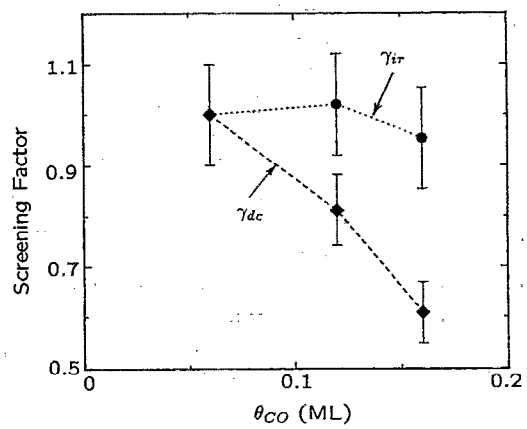

FIG. 11. Data showing the effect of coadsorbed H on the screening factors (●) γ_{IR} and (◆) γ_{dc} for CO on Pt(335). We assume that $\gamma_{IR}=1$ and $\gamma_{dc}=1$ at the lowest coverage, and that $\gamma_{IR}\propto\sqrt{S/\theta_{atop}}$ and $\gamma_{dc}\propto(d\nu/dE)$.

An increase in α_v with θ_{CO} was predicted by Ueba,[101] although the largest increase shown in his paper is only 13% at 1 ML. We are not aware of previous experimental evidence for this effect. The IR spectra of CO on Cu(100) and Ru(100) are well fit[105] by a dipole–dipole coupling model that assumes that α_v is coverage-independent.

Standard models of dipole coupling,[54,105] together with the assumption that all the coverage-dependence of $(d\nu/dE_{loc})$ is due to α_v, predict

$$S(\theta_{CO})\propto(\gamma_{IR})^2\alpha_v(\theta_{CO})\theta_{atop},$$
$$\left(\frac{d\nu}{dE}\right)(\theta_{CO})\propto\gamma_{dc}\sqrt{\frac{\alpha_v(\theta_{CO})}{\alpha_v(0)}}\left(\frac{d\nu}{dE}\right)(0), \tag{3}$$

where γ_{dc} is the screening factor for the static field and γ_{IR} is an effective IR screening factor.[105] Dipole-coupling theory[54,105] predicts $\gamma_{IR}\simeq\gamma_{dc}$ for CO. (Previous derivations have been for a system with only one CO species; with multiple species, γ_{IR} and γ_{dc} are modified, but these conclusions are still correct.[106]) We find, however, that for CO on Pt(335) γ_{dc} varies more rapidly with θ_{CO} than does γ_{IR}, similar to the results of Luo *et al.*[54] for CO on Pt(111). Figure 11 shows γ_{IR} and γ_{dc} calculated from Eq. (3), assuming $\alpha_v(\theta_{CO})$ and $\theta_{atop}/\theta_{CO}$ are constant and $\gamma_{IR}=\gamma_{dc}=1$ at the lowest coverage. If we instead take $\theta_{atop}/\theta_{CO}$ from Ref. 11, the discrepancy between γ_{IR} and γ_{dc} is even more pronounced. Allowing a coverage-dependent α_v will change the values of γ_{IR} and γ_{dc} in Fig. 11, but will not affect the disagreement between them. Either dipole coupling theory is inadequate for the calculation of E_{loc}, or $(d\nu/dE_{loc})$ exhibits coverage-dependence beyond that due to α_v.

The dependence of the C–O stretch frequency on work function, which is known from the experiments surveyed in Sec. V A and expected from Ueba's theory,[101] explains the small $\Delta\nu$ of CO vs θ_H. In particular, $\Delta\nu_{chem} \propto \Delta\Phi$. The maximum H-induced $\Delta\Phi$ for Pt(*S*)[6(111)×(100)] is[107] 0.08 eV; we assume similar behavior for our surface, Pt(*S*)[4(111)×(100)]. The H-induced $\Delta\Phi$ is then proportional to θ_H at step sites and reaches 0.08 eV when all step sites are filled. With 0.06 ML CO, 21% of the step sites are blocked from H occupation so the maximum H-induced $\Delta\Phi$ is 0.06 eV. If we assume that $\Delta\Phi$ from θ_{CO} and θ_H have the same effect on ν and use $(d\nu/d\Phi)=30$ cm^{-1}/eV, then $\Delta\nu=2.0$ cm^{-1}, more than half the observed shift. Since the measured $\Delta\Phi$ is an average over the surface, the $\Delta\Phi$ at the edge, and therefore the actual H-induced frequency shift, could be significantly larger. This suggests that most, and perhaps all of the observed $\Delta\nu$ could be caused by the H-induced $\Delta\Phi$, rather than by changes in local θ_{CO}.

Figure 7 shows a slight decrease in ν for θ_H above 0.3 ML for the two lowest θ_{CO}. (For $\theta_{CO}=0.16$ ML we were not able to reach such high θ_H.) At the highest θ_H, ν was 1973 ± 1 cm^{-1} with $\theta_{CO}=0.06$ ML and 1975 ± 1 cm^{-1} with $\theta_{CO}=0.12$ ML. Taking into account the H-induced chemical shift, these frequencies are close to that of an isolated atop CO molecule on the H-saturated edge (at $\theta_H=0$ the singleton frequency[7] ~1968 cm^{-1}). This is consistent with our model since at high θ_H nearly all of the atop CO has been shifted to bridge sites. As the population of atop CO decreases its dipole interaction also decreases. This reduces ν for the CO that remains.

Comparison of the data of $(d\nu/dE)$ vs θ_{CO} with the data of $(d\nu/dE)$ vs θ_H also suggests that the local density of CO that contributes to the IR spectrum is independent of θ_H. At each θ_{CO} in Fig. 7, a straight line was fit to the data of $(d\nu/dE)$ vs θ_H. The fit, expressed in terms of the effect of θ_{CO} on $(d\nu/dE)$, sets a limit to the effect of θ_H on local θ_{CO}. The estimated change in local θ_{CO} is 0–0.02 ML, consistent with the observed CO being in *the same local environment* at all but the highest H coverages.

C. Comparison with electrochemical experiments

Our experiments measure $(d\nu/dE)$ where E is externally applied in vacuum. Electrochemical experiments measure $(d\nu/d\phi)$, where ϕ is the potential of the sample relative to a reference electrode. As discussed in Sec. V A, to explain both $(d\nu/dE)$ measured in vacuum and $(d\nu/d\phi)$ measured in an aqueous electrolyte for CO on Pt(111), the local E-field in the compact double-layer must be a factor 2 larger than predicted by two different models. However, as solvent and solute are changed there is good correlation between $(d\nu/d\phi)$ and the expected $(dE_{loc}/d\phi)$ in the compact double layer.

Our experiment also finds a discrepancy between $(d\nu/dE)$ in vacuum and $(d\nu/d\phi)$ in an aqueous electrolyte. In the electrochemical experiments of Kim *et al.*[5,6] with CO on Pt(335) in 0.1 M $HClO_4$, $(d\nu/d\phi)$ for atop CO was found to depend on ϕ and θ_{CO}. At low θ_{CO}, there is a sharp transition in $(d\nu/d\phi)$ at $\phi \sim -0.1$ V (vs the saturated Calomel electrode). With $\phi < -0.1$ V, $(d\nu/d\phi)$ is zero. With $\phi > -0.1$ V, $(d\nu/d\phi) \sim 75$ cm^{-1}/V. At saturation θ_{CO}, the transition has disappeared and $(d\nu/d\phi)=33$ cm^{-1}/V over the entire potential range. A decrease in Stark tuning rate as θ_{CO} increases is seen both in the vacuum and electrochemical experiments. However, to explain the $(d\nu/d\phi)$ seen in the electrochemical experiment at low θ_{CO} (and for $\phi > -0.1$ V) with $(d\nu/dE)$ measured in vacuum at low θ_{CO}, we would need to have $(dE/d\phi)=0.85$ (V/Å)/V. In contrast, models of the compact double layer discussed in Sec. V A suggest that $(dE/d\phi) \sim 0.28$ (V/Å)/V. These two estimates of $(dE/d\phi)$ differ by a factor 3.0.

The sharp transition of $(d\nu/d\phi)$ in the electrochemical experiment at $\phi \sim -0.1$ V coincides with a peak in the cyclic voltammogram of the Pt(335) electrode. The peak is ascribed to H adsorption at the step edge.[108] Various models of H adsorption on single-crystal Pt have been proposed.[109] One interpretation of the electrochemical experiment is that coadsorbed H reduces CO's $(d\nu/d\phi)$ to zero. In contrast, in our vacuum experiment coadsorbed H has no effect on CO's $(d\nu/dE)$. This difference is very surprising.

VI. SUMMARY

We have investigated the coadsorption of H and CO on the step edges of Pt(335). On Pt(335), H and CO form compact mixed H/CO islands, within which the CO occupies only bridge sites. The mixed islands coexist with a pure CO phase that is largely unaffected by H. A similar mixed phase has been observed previously[34] for coadsorbed CO and H on polycrystalline Pt. In contrast, H and CO segregate completely on the structurally similar Pt(112) surface.[15] The Pt(112) surface used in that experiment also gave, with low H coverage and no CO, an anomalously low-temperature thermal desorption peak from edge H.

The Stark tuning rate that we measure for CO on Pt(335) is consistent with earlier measurements[9] in vacuum and with theoretical prediction, but is a factor 3.0 too small to explain $(d\nu/d\phi)$ for CO on Pt(335) in the electrochemical experiments of Kim *et al.*[5,6] Also, we find that H does not affect the Stark tuning rate of CO on Pt(335) in vacuum, but H is able to completely suppress $(d\nu/d\phi)$ in the electrochemical experiments.

Our evidence for an increase in the vibrational polarizability of CO with increasing CO coverage lends qualitative support to Ueba's theory of coadsorbate effects.[101] The small shift of CO's resonant frequency with θ_H is also roughly consistent with the dependence of frequency on work function expected both from theory and from previous experiments.

ACKNOWLEDGMENTS

We would like to thank Galen Fisher for helpful conversations. Acknowledgment is made to the donors of the Petroleum Research Fund, administered by the American Chemical Society, for partial support of this work. This material is based on work partially supported by the National Science Foundation under Grant No. DMR-9201077.

[1] K. C. Taylor, in *Catalysis Science and Technology*, edited by J. R. Anderson and M. Boudart (Springer, Berlin, 1984), Vol. 5, Chap. 2, pp. 119–170.
[2] G. Baier, V. Schüle, and A. Vogel, Appl. Phys. A **57**, 51 (1993).
[3] K. Christmann, G. Ertl, and T. Pignet, Surf. Sci. **54**, 365 (1976).
[4] K. Christmann, Surf. Sci. Rep. **9**, 1 (1988).
[5] C. S. Kim, W. J. Tornquist, and C. Korzeniewski, J. Phys. Chem. **97**, 6484 (1993).
[6] C. S. Kim, C. Korzeniewski, and W. J. Tornquist, J. Chem. Phys. **100**, 628 (1994).
[7] B. E. Hayden, K. Kretzschmar, A. M. Bradshaw, and R. G. Greenler, Surf. Sci. **149**, 394 (1985).
[8] J. S. Somers, T. Lindner, M. Surman, A. M. Bradshaw, G. P. Williams, C. F. McConville, and D. P. Woodruff, Surf. Sci. **183**, 576 (1987).
[9] D. K. Lambert and R. G. Tobin, Surf. Sci. **232**, 149 (1990). Recent unpublished data shows that $(d\nu/dE)$ for terrace CO on Pt(335) is actually larger than we saw here.
[10] J. S. Luo, R. G. Tobin, D. K. Lambert, F. T. Wagner, and T. E. Moylan, J. Electron Spectrosc. Relat. Phenom. **54/55**, 469 (1990).
[11] J. S. Luo, R. G. Tobin, D. K. Lambert, G. B. Fisher, and C. L. DiMaggio, Surf. Sci. **274**, 53 (1992).
[12] J. Xu, P. Henriksen, and J. T. Yates, Jr., J. Chem. Phys. **97**, 5250 (1992).
[13] J. Xu and J. T. Yates, Jr., J. Chem. Phys. **99**, 725 (1993).
[14] J. S. Luo, R. G. Tobin, D. K. Lambert, G. B. Fisher, and C. L. DiMaggio, J. Chem. Phys. **99**, 1347 (1993).
[15] M. A. Henderson and J. T. Yates, Jr., Surf. Sci. **268**, 189 (1992).
[16] E. Hahn, A. Frike, H. Röder, and K. Kern, Surf. Sci. **297**, 19 (1993).
[17] J. T. Yates, Jr. (private communication).
[18] D. K. Lambert, Appl. Opt. **27**, 3744 (1988).
[19] D. K. Lambert, J. Chem. Phys. **89**, 3847 (1988).
[20] K. Christmann and G. Ertl, Surf. Sci. **60**, 365 (1976).
[21] B. Klötzer and E. Bechtold, Surf. Sci. **295**, 374 (1993).
[22] C. S. Shern, Surf. Sci. **264**, 171 (1992).
[23] M. A. Henderson, A. Szabó, and J. T. Yates, Jr., J. Chem. Phys. **91**, 7245 (1989).
[24] B. Poelsema, G. Mechtersheimer, and G. Comsa, Surf. Sci. **111**, 519 (1981).
[25] K. E. Lu and R. R. Rye, Surf. Sci. **45**, 677 (1974).
[26] D. M. Collins and W. E. Spicer, Surf. Sci. **69**, 85 (1977).
[27] C.-M. Chan and W. H. Weinberg, Appl. Surf. Sci. **1**, 377 (1978).
[28] V. H. Baldwin, Jr. and J. B. Hudson, J. Vac. Sci. Technol. **8**, 49 (1971).
[29] K. Kawasaki, T. Kodama, H. Miki, and T. Kioka, Surf. Sci. **64**, 349 (1977).
[30] J. H. Craig, Jr., Surf. Sci. **111**, L695 (1981).
[31] J. H. Craig, Jr., Appl. Surf. Sci. **10**, 315 (1982).
[32] J. M. White, J. Phys. Chem. **87**, 915 (1983).
[33] D. E. Peebles, J. R. Creighton, D. N. Belton, and J. M. White, J. Catal. **80**, 482 (1983).
[34] K. A. Thrush and J. M. White, Appl. Surf. Sci. **24**, 108 (1985).
[35] E. G. Seebauer and L. D. Schmidt, Chem. Phys. Lett. **123**, 129 (1986).
[36] S. L. Bernasek, K. Lenz, B. Poelsema, and G. Comsa, Surf. Sci. **183**, L319 (1987).
[37] K. Lenz, B. Poelsema, S. L. Bernasek, and G. Comsa, Surf. Sci. **189/190**, 431 (1987).
[38] D. Hoge, M. Tüshaus, and A. M. Bradshaw, Surf. Sci. **207**, L935 (1988).
[39] D. H. Parker, D. A. Fisher, J. Colbert, B. E. Koel, and J. L. Gland, Surf. Sci. **258**, 75 (1991).
[40] J. M. White and S. Akhter, CRC Crit. Rev. Solid State Mater. Sci. **14**, 131 (1988).
[41] D. W. Goodman, J. T. Yates, Jr., and T. E. Madey, Surf. Sci. **93**, L135 (1980).
[42] L. Westerlund, J. Jönsson, and S. Andersson, Surf. Sci. **199**, 109 (1988).
[43] J. Bauhofer, M. Hock, and J. Küppers, J. Electron Spectrosc. Relat. Phenom. **44**, 55 (1987).
[44] J. G. Love, S. Haq, and D. A. King, J. Chem. Phys. **97**, 8789 (1992).
[45] M. L. Burke and R. J. Madix, J. Am. Chem. Soc. **113**, 1475 (1991).
[46] L. J. Richter, B. A. Gurney, and W. Ho, J. Chem. Phys. **86**, 477 (1987).
[47] H. Wang, R. G. Tobin, D. K. Lambert, G. B. Fisher, and C. L. DiMaggio (unpublished).
[48] T. E. Madey, J. T. Yates, Jr., A. M. Bradshaw, and F. M. Hoffmann, Surf. Sci. **89**, 370 (1979).
[49] P. Hofmann, S. R. Bare, N. V. Richardson, and D. A. King, Solid State Commun. **42**, 645 (1982).
[50] M. D. Alvey, M. J. Dresser, and J. T. Yates, Jr., Surf. Sci. **165**, 447 (1986).
[51] J. R. Smith, S. C. Ying, and W. Kohn, Phys. Rev. Lett. **30**, 610 (1973).
[52] P. J. Feibelman and D. R. Hamann, Surf. Sci. **182**, 411 (1987).
[53] D. F. Ogletree, M. A. Van Hove, and G. A. Somorjai, Surf. Sci. **173**, 351 (1986).
[54] J. S. Luo, R. G. Tobin, and D. K. Lambert, Chem. Phys. Lett. **204**, 445 (1993).
[55] E. Ruckenstein and T. Halachev, Surf. Sci. **122**, 422 (1982).
[56] M. D. Thompson and H. B. Huntington, Surf. Sci. **116**, 522 (1982).
[57] J. Martí and D. M. Bishop, J. Chem. Phys. **99**, 3860 (1993).
[58] P. S. Bagus, C. J. Nelin, W. Müller, M. R. Philpott, and H. Seki, Phys. Rev. Lett. **58**, 559 (1987).
[59] P. S. Bagus, C. J. Nelin, K. Hermann, and M. R. Philpott, Phys. Rev. B **36**, 8169 (1987).
[60] P. S. Bagus and G. Pacchioni, Surf. Sci. **236**, 233 (1990).
[61] M. Head-Gordon and J. C. Tully, Chem. Phys. **96**, 3939 (1993).
[62] C. W. Bauschlicher, Jr., Chem. Phys. Lett. **118**, 307 (1985).
[63] J. L. Andrés, M. Duran, A. Lledós, and J. Bertrán, Chem. Phys. **151**, 37 (1991).
[64] J. L. Andrés, J. Martí, M. Duran, A. Lledós, and J. Bertrán, J. Chem. Phys. **95**, 3521 (1991).
[65] J. Martí, A. Lledós, J. Bertrán, and M. Duran, J. Comp. Chem. **13**, 821 (1992).
[66] Z. Xu, J. T. Yates, Jr., L. C. Wang, and H. J. Kreuzer, J. Chem. Phys. **96**, 1628 (1992).
[67] D. M. Bishop, J. Chem. Phys. **98**, 3179 (1993).
[68] K. Hermansson, J. Chem. Phys. **99**, 861 (1993).
[69] D. K. Lambert, Solid State Commun. **51**, 297 (1984).
[70] M. Tüshaus, E. Schweizer, P. Hollins, and A. M. Bradshaw, J. Electron Spectrosc. Rel. Phenom. **44**, 305 (1987).
[71] K. Horn and J. Pritchard, J. Phys. (Paris) **38**, C4-164 (1977).
[72] G. Ertl, M. Neumann, and K. M. Streit, Surf. Sci. **64**, 393 (1977).
[73] P. R. Norton, J. W. Goodale, and E. B. Selkirk, Surf. Sci. **83**, 189 (1979).
[74] I. Yamamoto and T. Nanba, Surf. Sci. **202**, 377 (1988).
[75] Z. Xu, M. G. Sherman, J. T. Yates, Jr., and P. R. Antoniewicz, Surf. Sci. **276**, 249 (1992).
[76] F. Kitamura, M. Takeda, M. Takahashi, and M. Ito, Chem. Phys. Lett. **142**, 318 (1987).
[77] L.-W. H. Leung, A. Wieckowski, and M. J. Weaver, J. Phys. Chem. **92**, 6985 (1988).
[78] N. Furuya, S. Motoo, and K. Kunimatsu, J. Electroanal. Chem. **239**, 347 (1988).
[79] S.-C. Chang, L.-W. H. Leung, and M. J. Weaver, J. Phys. Chem. **93**, 5341 (1989).
[80] F. Kitamura, M. Takahashi, and M. Ito, Surf. Sci. **223**, 493 (1989).
[81] S.-C. Chang and M. J. Weaver, J. Chem. Phys. **92**, 4582 (1990).
[82] Y. Kinomoto, S. Watanabe, M. Takahashi, and M. Ito, Surf. Sci. **242**, 538 (1991).
[83] S.-C. Chang and M. J. Weaver, J. Phys. Chem. **95**, 5391 (1991).
[84] S.-C. Chang, X. Jiang, J. D. Roth, and M. J. Weaver, J. Phys. Chem. **95**, 5378 (1991).
[85] X. Jiang and M. J. Weaver, Surf. Sci. **275**, 237 (1992).
[86] M. J. Weaver, Appl. Surf. Sci. **67**, 147 (1993).
[87] M. R. Anderson, D. Blackwood, and S. Pons, J. Electroanal. Chem. **256**, 387 (1988).
[88] M. R. Anderson, D. Blackwood, T. G. Richmond, and S. Pons, J. Electroanal. Chem. **256**, 397 (1988).
[89] J. G. Love and A. J. McQuillan, J. Electroanal. Chem. **274**, 263 (1989).
[90] J. D. Roth, S.-C. Chang, and M. J. Weaver, J. Electroanal. Chem. **288**, 285 (1990).
[91] A. E. Russell, S. Pons, and M. R. Anderson, Chem. Phys. **141**, 41 (1990).
[92] A. E. Russell, D. Blackwood, M. R. Anderson, and S. Pons, J. Electroanal. Chem. **304**, 219 (1991).
[93] K. Ashley, M. G. Samant, H. Seki, and M. R. Philpott, J. Electroanal. Chem. **270**, 349 (1989).
[94] L.-W. H. Leung, S.-C. Chang, and M. J. Weaver, J. Chem. Phys. **90**, 7426 (1989).
[95] M. R. Anderson and J. Huang, J. Electroanal. Chem. **318**, 335 (1991).
[96] J. D. Roth and M. J. Weaver, Langmuir **8**, 1451 (1992).
[97] C. M. Mate, C.-T. Kao, and G. A. Somorjai, Surf. Sci. **206**, 145 (1988).
[98] J. O'M. Bockris, M. A. V. Devanathan, and K. Müller, Proc. R. Soc. London Ser. A **274**, 55 (1963).
[99] D. K. Lambert, Phys. Rev. Lett. **50**, 2106 (1983); **51**, 2233 (E) (1983).
[100] R. P. Feynman, Phys. Rev. **56**, 340 (1939).
[101] H. Ueba, Surf. Sci. **188**, 421 (1987).

[102] N. K. Ray and A. B. Anderson, J. Phys. Chem. **86**, 4851 (1982).
[103] H. S. Luftman and J. M. White, Surf. Sci. **139**, 369 (1984).
[104] S. Holloway and J. K. Nørskov, J. Electroanal. Chem. **161**, 193 (1984).
[105] B. N. J. Persson and R. Ryberg, Phys. Rev. B **24**, 6954 (1981).
[106] H. Wang and R. G. Tobin (unpublished).
[107] D. M. Collins and W. E. Spicer, Surf. Sci. **69**, 114 (1977).
[108] A. Rodes, K. El Achi, M. A. Zamakhchari, and J. Clavilier, J. Electroanal. Chem. **284**, 245 (1990).
[109] A. Wieckowski, P. Zelenay, and K. Varga, J. Chim. Phys. **88**, 1247 (1991).